Joint Pathology Center

Veterinary Pathology Services

WEDNESDAY SLIDE CONFERENCE 2016-2017

C o n f e r e n c e 9

2 November 2016

Victoria Hoffmann, VMD, DACVP
Division of Veterinary Resources
National Institutes of Health
Bethesda, MD

CASE I: 14L-2800B (JPC 4066544).

Signalment: Adult, female, European rabbit (*Oryctolagus cuniculus*).

History: A member of the public found the collapsed rabbit in a field close to their home and presented it to the local veterinary practice where the rabbit was euthanized on humane grounds.

Gross Pathology: The eyelids were bilaterally severely swollen with an exudate lightly adhered to the surface. The nostrils had a bilateral discharge. The vulva was severely swollen.

Laboratory results: N/A

Histopathologic Description: The slide consists of a section of haired skin and vulva including mucocutaneous junction. There is diffuse moderate to severe hyperplasia of the mucosal epithelium. Multifocally epithelial cells throughout all the layers of the epithelium are enlarged, often degenerate, with clear intracytoplasmic spaces (intracellular edema). Often,

epidermal cells contain large, approximately 15 to 20 µm diameter, round to oval, homogenous, brightly eosinophilic cytoplasmic inclusions. The same inclusions may also be observed in sloughed epithelial cells and within the thickened stratum corneum showing moderate orthokeratotic hyperkeratosis. Randomly scattered throughout the epidermis there are

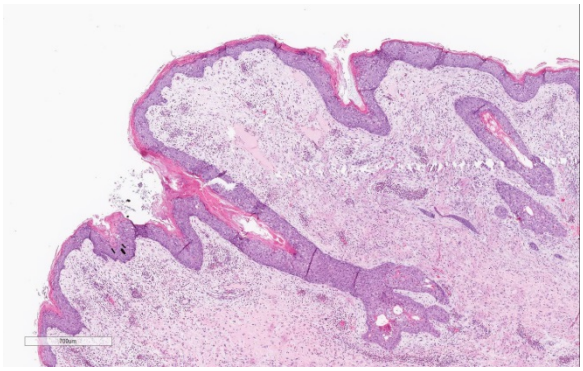

Vulva, mucocutaneous junction, rabbit. The epidermis is markedly and diffusely hyperplastic and there is overlying moderate orthokeratotic hyperkeratosis. The dermis is expanded by edema and is hypercellular. (HE, 4X)

occasional keratinocytes with hyper-eosinophilic cytoplasm and karyorrhectic nuclei (single cell necrosis). There are diffusely scattered basophilic granules within keratinocytes (keratohyaline granules) of the stratum granulosum and rarely deep within the stratum basale (dyskeratosis). Multifocally, the epithelial cells of the vaginal mucosa are expanded by a single large clear vacuole (intracellular edema / ballooning degeneration).

Diffusely the lamina propria is characterized by a loosely arranged slightly basophilic myxoid matrix admixed with edematous areas. Multifocally in the dermis there are plump elongated to polygonal fibroblasts with stellate processes. These cells have finely granular basophilic cytoplasm, a single distinct, round to elongate and centrally placed large nucleus with finely stippled chromatin and a single evident nucleolus. Anisocytosis and anisokaryosis are moderate and mitotic figures are rare.

Within the superficial dermis and surrounding the blood vessels in the deeper dermis there are moderate, multifocal to coalescing aggregates of lymphocytes, plasma cells, heterophils, and macrophages. Occasionally, in the superficial dermis, the inflammatory process is predominately heterophilic.

Contributor's Morphologic Diagnosis: 1. Vulva, mucocutaneous junction: Diffuse, subacute, moderate to severe epidermal hyperplasia with intracellular edema and intracytoplasmic viral inclusions.

2. Vulva, mucocutaneous junction: Multifocal to coalescing, subacute, moderate lymphoplasmacytic and heterophilic proliferative dermatitis and sub-mucosal proliferation with diffuse myxoid changes and edema.

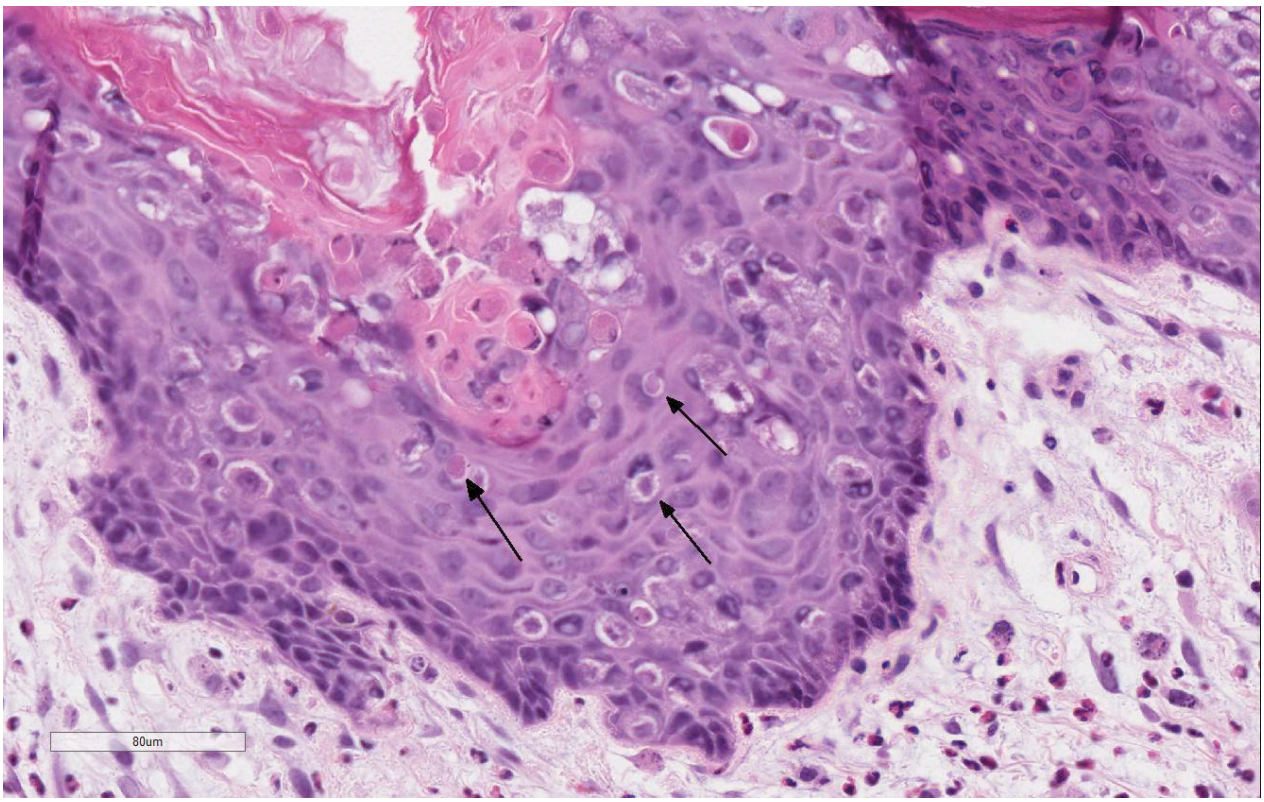

Vulva, rabbit. Scattered keratinocytes at all level of the epidermis contain 2-4um round eosinophilic viral inclusions (arrows), and multifocally, variable degrees of intracytoplasmic edema (ballooning degeneration) or apotptosis. (HE, 296X)

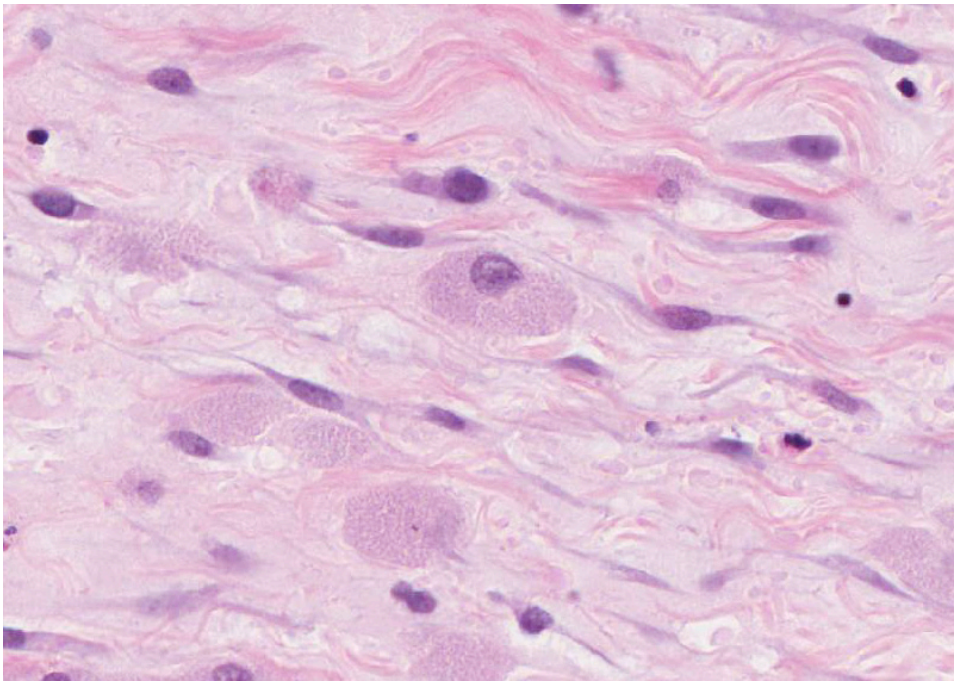

Vulva, rabbit. The dermis is markedly edematous and contains numerous polygonal "myxoma" cells with abundant granular amphophilic cytoplasm and anisokaryotic nuclei. (HE, 332X)

Contributor's Comment: Myxomatosis is a common, worldwide distribution disease of rabbits and is now endemic in the wild rabbit population in Europe. Hares may be carriers of the infection but very rarely exhibit clinical signs.[2] Originally myxomatosis was introduced in Europe to control the wild rabbit population.[9] Initially the disease had a very high mortality rate, but due to natural selection the wild rabbit population began to develop immunity to the disease and mortality rate is now approximately 25% in the European rabbits.[9]

Myxomatosis is caused by the Myxoma virus, a leporipoxvirus from the family of poxviruses.[6] Transmission of the virus requires a mosquito or flea vector, but it is possible for the virus to spread by direct contact. Due to transmission routes, domestic rabbits, especially the ones kept outdoors are at risk of contracting the virus from the wild rabbit population and therefore a vaccine has been developed.

There are two recognized forms of the disease: the classical, nodular form (as in this case); and the respiratory, amyxomatous form of the disease. The nodular form is often transmitted by vector route and causes the classical swelling of the eyelids, nodules over the skin, and edema of the genitalia. Usually, there is ocular and nasal discharge associated with the disease. The infection causes a severe depression of the host's immune system causing secondary infections to take hold and often the secondary infections are the ultimate cause of death. The amyxomatous form is usually due to a mild or attenuated strain of the virus;[6] this causes respiratory signs and rarely nodular lesions.

Other skin disease that may be confused for myxomatosis is Shope fibroma caused by the rabbit Shope fibroma virus (SFV, Leporipoxvirus). Shope fibroma virus induces discrete fibromas usually restricted to the distal limbs but occasionally may be found in the head.

JPC Diagnosis: Mucocutaneous junction, vulva: Atypical mesenchymal proliferation, diffuse, moderate, with epithelial and epidermal hyperplasia, ballooning degeneration, lymphoplasmacytic and heterophilic dermatitis, and epithelial intracytoplasmic eosinophilic inclusions, European rabbit, *Oryctolagus cuniculus*.

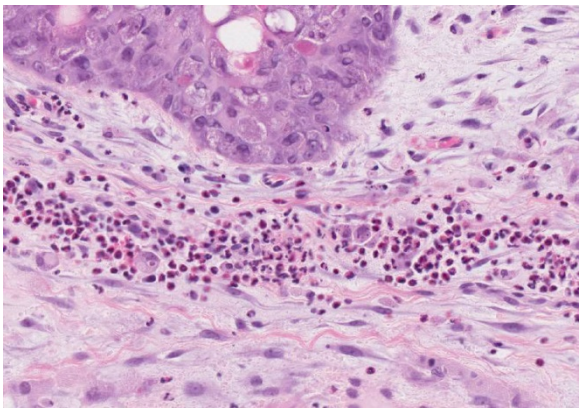

Vulva, rabbit. Superficial dermal vessels are surrounded by large numbers of heterophils which occasionally form dermal aggregates beneath the hyperplastic epidermis. (HE, 176X)

Conference Comment: Poxviruses are a large family of epitheliotropic double-stranded DNA viruses that cause several important cutaneous and systemic lesions in wild and domestic mammals, birds, and humans.[8] Most poxviruses cause a mild localized cutaneous lesion, but some can cause generalized systemic and fatal disease. An example of the latter is the rabbit myxoma virus, a member of the genus *Leporipoxvirus*, which can cause up to 90% mortality in naïve susceptible strains of wild rabbits.[2,8,9] However, through natural selection, genetically resistant strains of wild rabbits now have only about 25% mortality when infected with virulent strains of the virus in endemic areas.[9] Readers are encouraged to review 2012 Wednesday Slide Conference #2 Case 2 for a brief review of the fascinating history of this virus, and its use during attempted European rabbit (*Oryctolagus cuniculus*) eradication programs in Australia and France in the early 1950's.

Following inoculation, typically by an arthropod vector, susceptible rabbits develop localized skin tumors resembling fibromas caused by the rabbit (Shope) fibroma virus discussed above by the contributor.[3,9] Other characteristic gross lesions are pronounced gelatinous subcutaneous edema surrounding mucocutaneous junctions. In this case, the contributor noted severe swelling around the eyelids and vulva with nasal discharge grossly.[9]

While the microscopic staining of the tissue section of vulva is somewhat pale, this case nicely illustrates the classic histologic poxviral epithelial intracytoplasmic inclusions and ballooning degeneration.[8] In addition, there is a subepithelial proliferation of large stellate mesenchymal cells within a homogenous mucinous matrix. Conference participants also noted a moderate lymphoplasmacytic inflammatory infiltrate admixed with the atypical mesenchymal cells. In addition to being epitheliotropic, the myxoma virus is T-lymphocytotrophic and systemic spread occurs via lymphocytes and monocytes to draining lymph nodes.[9] Myxoma stellate cells are typically present in lymph nodes, bone marrow, spleen, and centrilobular areas of the liver. Degenerative and necrotizing lesions are usually confined to the lymphoid tissue in lymph nodes, lungs, and spleen with lymphoid depletion, particularly in the T-cell zones.[9]

Recently, there has been a great deal of interest in the rabbit myxoma virus as one of the promising new oncolytic viruses used in virotherapy for human cancer. Oncolytic viruses are engineered to preferentially infect and kill cancer cells while sparing normal host cells.[4,7] Several other oncolytic viruses originated from human pathogens (herpes simplex-1, measles, etc) and still retain some ability to replicate in normal host tissue. Myxoma virus is attractive to researchers because its pathogenicity is restricted to lagomorphs and thus it will not replicate or kill normal human host cells; but the virus does have significant oncolytic potential for a large variety of neoplasms in several animal species and humans.[4,7]

Contributing Institution:

University of Liverpool
Department of Veterinary Pathology, Leahurst Campus,
Chester High Road
Neston, England, United Kingdom
https://www.liv.ac.uk/vetpathology/

References:

1. Bangari DS, Miller MA, Stevenson GW, et. al. Cutaneous and systemic poxviral disease in red (*Tamiasciurus hudsonicus*) and gray (*Sciurus carolinensis*) squirrels. *Vet* Patho.l 2009; 46:667-672.
2. Barlow A., et al. Confirmation of myxomatosis in a European brown hare in Great Britain. *Vet Rec*. 2014; 175(3):75-6.
3. Berto-Moran A, Pacios I, Serrano E, Moreno S, Rouco C. Coccidian and nematode infections influence prevalence of antibody to myxoma and rabbit hemorrhagic disease viruses in European rabbits. *J Wildl Dis*. 2013; 49(1):10-17.
4. Chan WM, McFadden G. Oncolytic poxviruses. *Annu Rev Virol*. 2014; 1:119-141.
5. DiGiacomo RF, Mare CJ. Viral diseases. In: Manning PJ, Ringler DH, Newcomer CE, eds. *The Biology of the Laboratory Rabbit.* 2nd ed. San Diego, CA: Academic Press; 1994:178-180.
6. Kerr, P.J., et al., Myxoma virus and the Leporipoxviruses: An evolutionary paradigm. *Viruses*. 2015; **7**(3):1020-61.
7. Kinn VG, Hilgenberg VA, MacNeill AL. Myxoma virus therapy for human embryonal rhabdo-myosarcoma in a nude mouse model. *Oncolytic Virother*. 2016; 5:59-71.
8. Mauldin E, Peters-Kennedy J. Integumentary system. In: Maxie MG, ed. *Jubb, Kennedy, and Palmer's Pathology of Domestic Animals*. Vol 1. 6th ed. Philadelphia, PA:Elsevier; 2016:616-625.
9. Percy DH, Barthold SW. *Pathology of Laboratory Rodents and Rabbits*. rd ed. Ames, IA: Blackwell Publishing; 2016:261-263.

CASE II: DX16-0081 (JPC 4084542).

Signalment: Four-month-old female NOD.*Cg-Prkdc*^{scid}*Il2rg*^{tm1Wjl}/SzJ mouse, (*Mus musculus*).

History: Animal presented moribund after receiving a xenotransplant.

Gross Pathology: Discolored nodules were visible on the kidney. Secondary lymphoid tissues were markedly reduced in size consistent with the phenotype of the strain.

Laboratory results: Microbiology, Aerobic bacterial culture of both tympanic bullae:

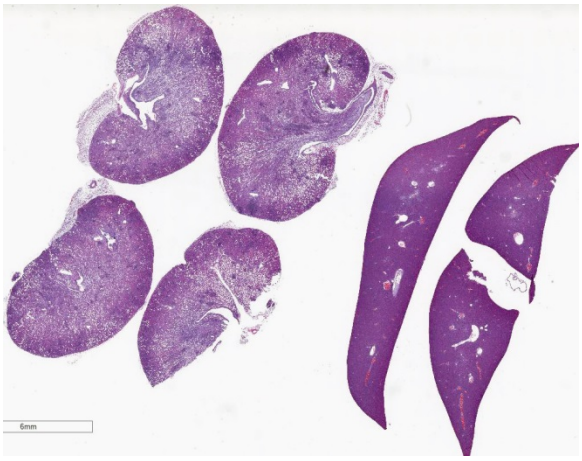

Kidney and liver, NOD mouse. The bisected kidneys show randomly scattered foci of cellular inflammation within the cortex and medulla. (HE, 5X)

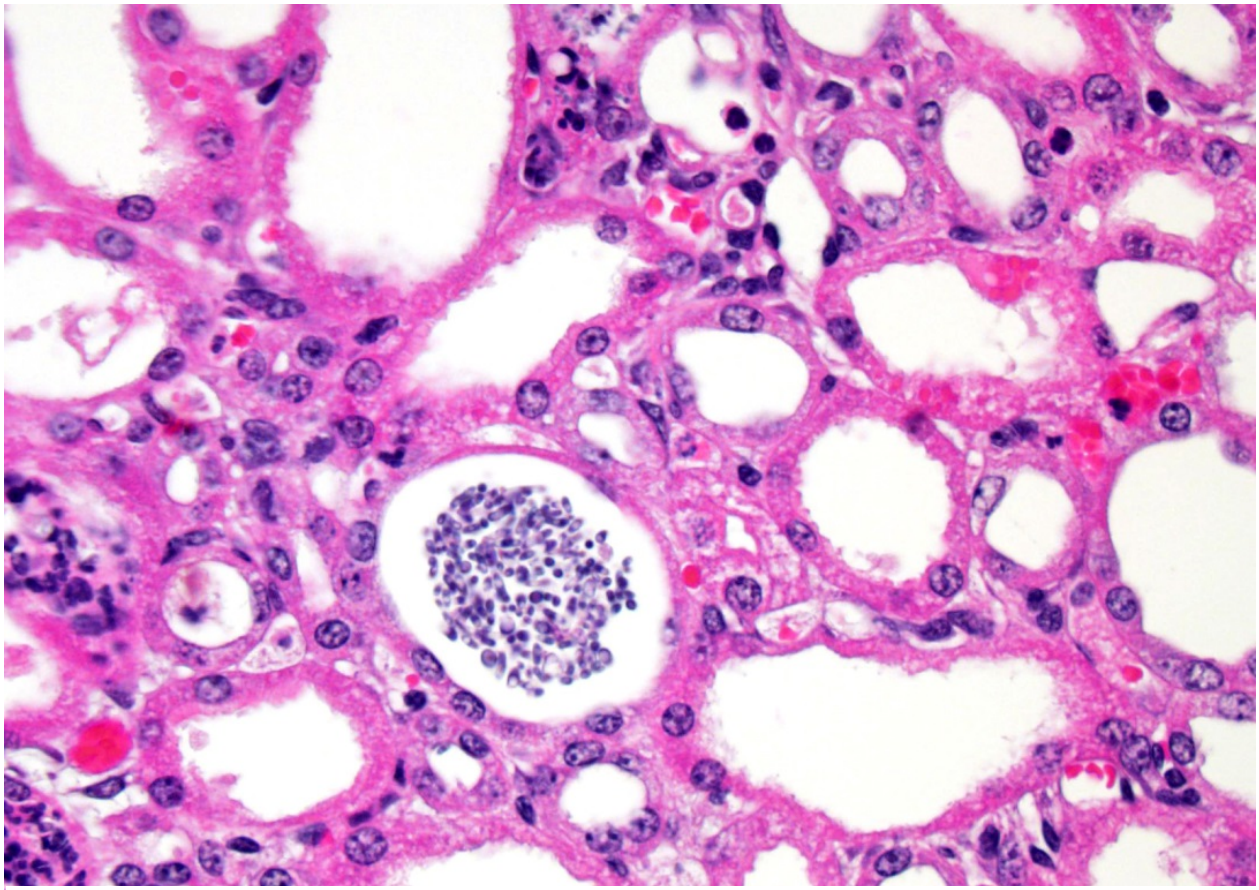

Kidney, NOD mouse. Numerous tubules contain large numbers of 3-6um thin-walled yeasts (blastospores). (HE, 400X)

Klebsiella pneumonia.

Microbiology, Aerobic bacterial culture of blood: *Staphylococcus xylosus*.

Histopathologic Description: There is marked, multifocal to coalescing neutrophilic inflammation and necrosis arranged in an embolic pattern and which distorts the overall structure of the kidneys as viewed subgrossly. Inflammation is centered on 0.5um wide X 8.0-10.0uM long fungal organisms that form non-branching hyphae and pseudohyphae. Organisms and the accompanying inflammatory response involve predominately vascular and perivascular, interstitial spaces and the tubules with limited extension into the kidney parenchyma. Affected renal tubules are variably ectatic and contain combinations of serocellular debris and acellular eosinophilic material. The renal interstitium is variably expanded by inflammation and reactive fibroblasts, especially where inflammation is present. The adjacent sections of liver are unremarkable.

Yeast forms are also observed in the following locations: Both ears, heart, and the stomach.

Contributor's Morphologic Diagnosis: Kidney: Tubulointerstitial nephritis, suppurative, bilateral, acute, severe with intratubular fungal organisms most consistent morphologically with *Candida albicans*.

Contributor's Comment: Non-obese diabetic (NOD)/severe combined immune

deficiency (SCID)/IL2rγnull (NSG) mice represent a severely immunocompromised mouse strain that is an important tool for xenotransplantation studies using patient-derived tissues. This strain is deficient in mature B cells, mature T cells, and natural killer (NK) cells. Additionally, macrophages and dendritic cells are defective regarding their functions.[5] While the severe immunodeficiency trait of the strain is useful for avoiding immune-mediated host rejection of foreign cells, this compromised status leaves NSG mice susceptible to a number of opportunistic pathogens. Three commonly encountered opportunistic pathogens of immuno-compromised laboratory mice are either observed in tissue lesions or are isolated from body fluids of this NSG mouse including *Candida albicans, K. pneumoniae* and *S. xylosus*.

Candida albicans, the organism observed in the renal lesions, is a common microbial component of the gastrointestinal tracts of mice and other species that is held in check by aspects of both the innate and adaptive immune responses.[3] The ability of different laboratory mouse strains and man to contain any disease that may be induced by *C. albicans* is often related to having the appropriate T-cell-directed phagocytic responses.[1] Interestingly the depletion of T lymphocytes in the human and mouse generally results only in a severe mucosal overgrowth of this yeast. Furthermore,

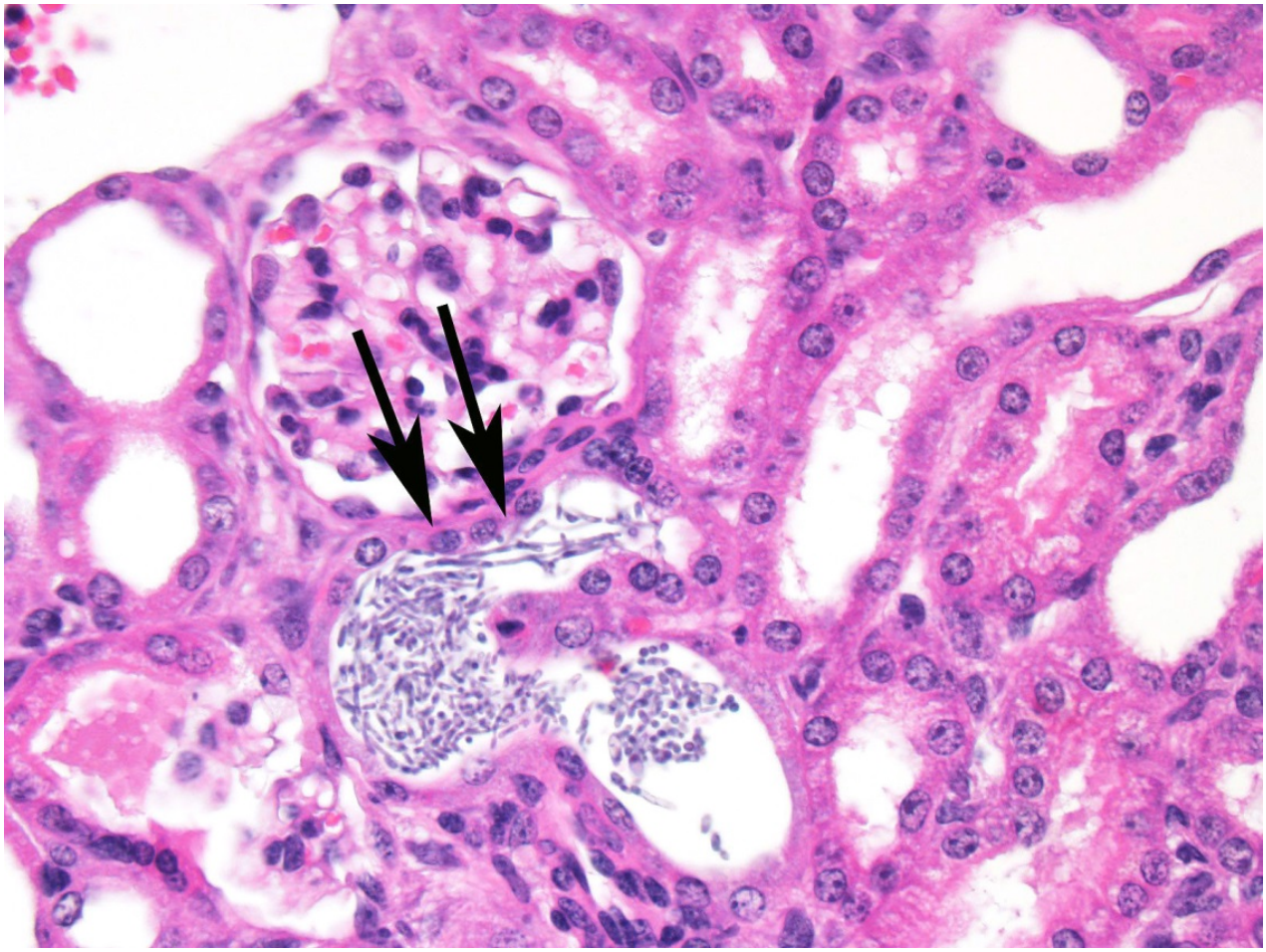

Kidney, NOD mouse. Within some tubules, yeasts have matured into pseudohyphae (arrows). (HE, 400X)

neither nude nor NOD-SCID mice have shown increased susceptibilities to developing systemic candidiasis, which indicate that the innate immune system offers protection, as well.[1] However, impaired NK cell function appears to be essential for immune-mediated signaling that shields against developing systemic candidiasis. Therefore, severely immuno-suppressed hosts, such as the NSG mouse, are uniquely susceptible to systemic disease induced by *C. albicans* infection.[4]

JPC Diagnosis: 1. Kidney: Pyelonephritis, suppurative, acute, multifocal, marked with pseudohyphae and yeast, NOD.*Cg-Prkdc*^{scid}*Il2rg*^{tm1Wjl}/SzJ mouse, *Mus musculus*.
2. Liver: No significant lesions

Conference Comment: In addition to being globally immuno-deficient and uniquely susceptible to a variety of opportunistic infections, non-obese diabetic (NOD)/ severe combined immune deficiency (SCID; NSG) mice are selectively bred as an animal model for type I diabetes mellitus (DM) in humans.[3] In NOD mice, DM develops as a result of spontaneously developing autoimmune insulitis in the pancreatic islets cells. The onset of DM is associated with a moderate glycosuria and a non-fasting hyperglycemia, which may be important for the proposed pathogenesis of this lesion discussed below.[3] As mentioned by the contributor, NOD-SCID mice have functional defects in macrophages, dendritic cells, natural killer (NK) cells, NKT cells, regulatory CD4+CD25+ cells, and are C5a deficient. The susceptibility of these mice to develop DM is much higher in a sterile environment.[3]

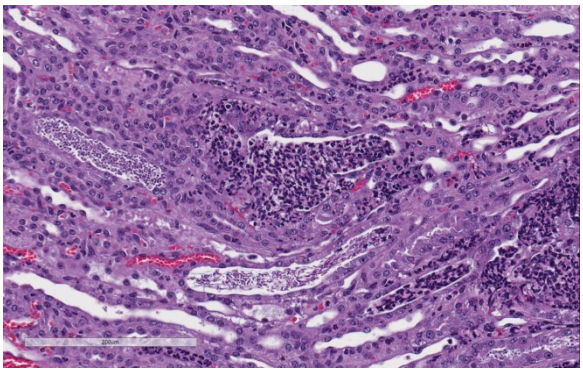

Kidney, NOD mouse. Adjacent tubules are filled with a mixture of yeast and large numbers of degenerate neutrophils. (HE, 200X)

Virulence of *C. albicans* is dependent on adherence of the organism to mucosal epithelial cells mediated by its virulence factor, adhesin. The important components of adhesins are agglutinin-like sequence (ALS) proteins and hypha-associated GPI-linked protein (Hwp1).[6,7] Superficial (localized) candidiasis produces relatively mild lesions in skin and mucous membranes while systemic (disseminated) candidiasis may involve any organ with the kidneys, heart valves, CNS and lungs most commonly affected. Immunosuppression, cytotoxic chemotherapy, diabetes mellitus, long-term glucocorticoid therapy, prolonged use of broad-spectrum antibiotics, or disruption of mucosal barriers predispose to infection. In addition, *C. albicans* can exist as yeast, pseudohyphae, or true hyphae depending on environmental conditions and temperature. This polymorphism enables *C. albicans* to infect a variety of tissues throughout the body.[6,7] The yeast form has been implicated in disseminated systemic infection while hyphae and pseudohyphae have stronger adherence and invasiveness due to the expression of ALS adhesins, catalases, and protein hydrolases, such as secreted aspartyl proteinases (SAP), which also supply the pathogen nutrients through protein degradation.[6,7]

Conference participants noted large numbers of *Candida* sp. pseudohyphae and yeast admixed with and surrounded by suppurative inflammation in the renal pelvis as well as filling and expanding renal

tubules in both the cortex and medulla. Occasionally tubules rupture and the inflammation extends into the adjacent renal interstitium. Participants agreed that this pattern of inflammation is consistent with pyelonephritis and retrograde extension of exudate into the renal tubules and renal parenchyma. The most common cause of pyelonephritis is via ascending infection from the lower urinary tract.[2] Opportunistic pathogens, such as *Candida albicans*, can commonly ascend into the kidney from the lower urinary tract, especially if there is glycosuria in a severely immuno-compromised and diabeteic animal. Females are predisposed to ascending urinary tract infections and pyelonephritis due to their relatively shortened urethra compared to males.[2] Alternatively, hematogenous suppurative and embolic nephritis usually results in multiple microabscesses within the glomeruli, multifocal vascultitis, and

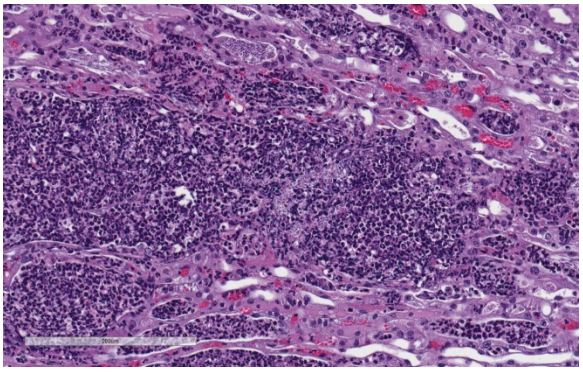

Kidney, NOD mouse. There is multifocal rupture of yeast- and neutrophil-laden tubules with extension of the inflammation into the adjacent interstitium. (HE, 200X)

hemorrhage within the medulla. In this case, conference participants noted perivascular in-flammation, but not significant vasculitis or glomerular lesions.[2]

Contributing Institution:
Veterinary Pathology Core Laboratory
St. Jude Children's Research Hospital
262 Danny Thomas Place
Memphis, TN, 38105-3678
https://www.stjude.org/research/departments-divisions/pathology

References:

1. Ashman, R, Farah, C, Wanasaengsakul, S, Hu, Y, Pang, G, Clancy, R. Innate versus adaptive immunity in *Candida albicans* infection. *Immunol Cell Biol*. 2004; 82(2):196-204.
2. Percy DH, Barthold SW. *Pathology of Laboratory Rodents and Rabbits*, 4th ed. Ames, IA: Blackwell Publishing; 2016:4,79.
3. Quintin J, Voigt J, Van der Voort R, et al. Differential role of NK cells against *Candida albicans* infection in immunocompetent or immunocompromised mice. *Eur J Immunol*. 2014; 44(8):2405-14.
4. Shultz L, Yoriko S, Najima Y, et al. Generation of functional human T-cell subsets with HLA-restricted immune responses in HLA class I expressing NOD/SCID/IL2rγ^{null} humanized mice. *Proc Natl Acad Sci USA*. 2010; 107:13022-13027.
5. Uzal FA, Plattner BL, Hostetter JM. Alimentary system. In: Maxie MG, ed. *Jubb, Kennedy, and Palmer's Pathology of Domestic Animals*. Vol 2. 6th ed. Philadelphia, PA:Elsevier; 2016:202.
6. Voon KC, Lee TY, Rusliza B, Chong PP. Dissecting *Candida albicans* infection from the perspective of *C. albicans* virulence and omics approaches on host-pathogen interaction: A review. *Int J Mol Sci*. 2016; 17:1643.

CASE III: Case #1 (JPC 4084692).

Signalment: Three-year-old, male, RCS rat (*Rattus norvegicus*).

History: The rat was kept as a non-treated animal in a long-term rat study. No clinical signs except coarse hair were found until the scheduled sacrifice at 152 weeks old.

Gross Pathology: A mass measured 40 x 30 x 15 mm, was observed in the anterior mediastinum, and adhered to the pleura of the lung. Small masses had found around main mass, and adhered to the lung and esophagus. The mass was soft, and the cut surface was milky white to yellow and grey-white.

Laboratory results: N/A

Histopathologic Description: Affecting approximately 80% of this section of thymus is an unencapsulated, poorly circumscribed, moderately cellular neoplasm composed of round to spindle-shaped cells arranged in sheets on a pre-existent fibrovascular stroma. Neoplastic cells have variably distinct cell borders, an abundant amount of lightly eosinophilic to amphophilic cytoplasm that is often obscured by fine eosinophilic granules. The nuclei of the tumor cells are generally centrally placed, round to elongate, with finely stippled chromatin, and 1-2 variably distinct nucleoli. Mitotic count averages about 1 per HPF. Almost all tumor cells have metachromatic granules when stained with toluidine blue stain. Immuno-histochemically, tumor cells are positive for c-kit, strongly positive for rat mast cell protease, and mostly negative for histamine as mast cell tumor markers. All tumor cells

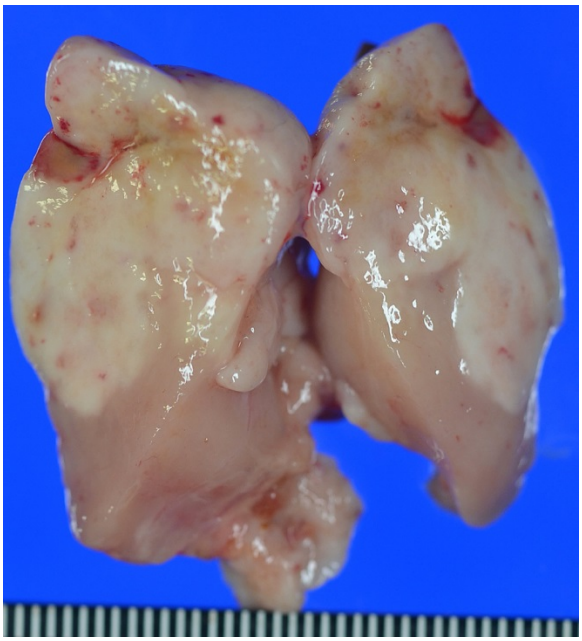

Anterior mediastinum, rat. A mass measured 40 x 30 x 15 mm, was observed in the anterior mediastinum, and adhered to the pleura of the lung. The mass was soft, and the cut surface was milky white to yellow and gray white in color (Photo courtesy of: Laboratory of Pathology, Faculty of Pharmaceutical Sciences, Setsunan University, 45-1 Nagaotohge-cho, Hirakata, Osaka 573-0101, Japan http://www.setsunan.ac.jp/~p-byori/)

are negative for cytokeratin AE1/AE3, and positive for vimentin. Ultrastructurally, the various sized granules contained homogeneous electron-dense material consistent with mast cell granules. The tumor metastasized and disseminated to the pleura of the lung and esophagus, and adventitia of the left ventricles and aorta.

The basophilic area at the periphery of the mass consists of a large number of lymphocytes and thymic epithelial cells similar to normal thymic tissue. Lympho-cytes in high cell density areas of epithelial cells are mostly a small cell type with coarse chromatin and fewer large lymphocytes. On the other hand, lymphocytes in low cell density areas of epithelial cells are nearly uniform medium-sized cell with fine stippled chromatin. Immunohistochemically, the thymic epithelial cells in high-cell-

Thymus, rat. 85% of the thymus (normal at left edge) is effaced by a neoplasm. (HE, 5X).

density areas exhibit positive cytokeratin 8 staining, which is expressed in thymic cortical epithelial cells. Thymic epithelial cells in low-cell-density areas are positive for cytokeratin 14 which is expressed in thymic medullary epithelial cells.

Contributor's Morphologic Diagnosis: Thymus: Malignant mast cell tumor with thymic epithelial hyperplasia

Contributor's Comment: This malignant tumor of thymic origin was located in the anterior mediastinum, invaded the adjacent thymus, and metastasized to the thoracic cavity. The tumor is characterized by a dense round cell proliferation, and has the features of a malignant round cell tumor. Neoplastic cells have intracytoplasmic metachromatic granules with toluidine blue stain and are strongly immunopositive for mast cell markers. Therefore, the tumor is diagnosed as a malignant mast cell tumor.

Mast cell tumor is a very common neoplasm of the skin in the dog and cat[5,6], and is composed of round cells with basophilic granules which are metachromatic when stained with toluidine blue. With regard to rodents, chemical and radiation-induced and spontaneous mast cell tumor have been reported in mice.[3,8] However, to our knowledge, mast cell tumors are extremely rare in rats. Rat mast cell tumors have only been reported in two case reports; and there are 12 cases/entries in the National Toxicology Program (NTP) pathology database.[2,3] Histopathologically, the mast cell tumors described in the two case reports originated in the thymus and in the eyelid, and they were characterized by a sheet-like proliferation of round cells with fine cytoplasmic eosinophilic granules. However, infiltration of eosinophils and an increase in collagen fibers are not observed, unlike in cases of these tumors in dogs and cats.[1,2,3,4] Because our case has similar morphologic features to previously reported cases, mast cell tumor in the rat may be characterized by eosinophilic granules in the cytoplasm. However, since this case has variable cell morphology and evidence of metastasis, the mast cell tumor in this case may have more malignant potential compared with previous reports.

This case is characterized by sheet-like proliferation of spindle to round cells with eosinophilic granules of various sizes. Differential diagnoses for the present tumor included thymoma, granular cell tumor, and globule leukocyte tumor. Thymoma, an epithelial tumor, is easily distinguishable from a round cell tumor; however, the patterns of cellular proliferation observed in the present case resemble that seen in tumors of epithelial origin, making the rat

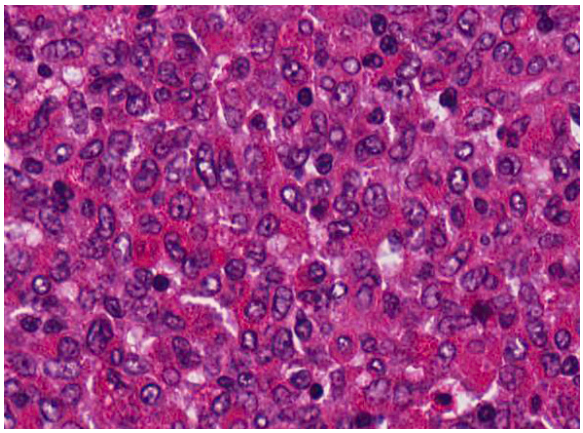

Thymus, rat. The neoplasm is composed of sheets of round cells with brightly eosinophilic granules and irregularly indented nuclei. (HE, 400X).

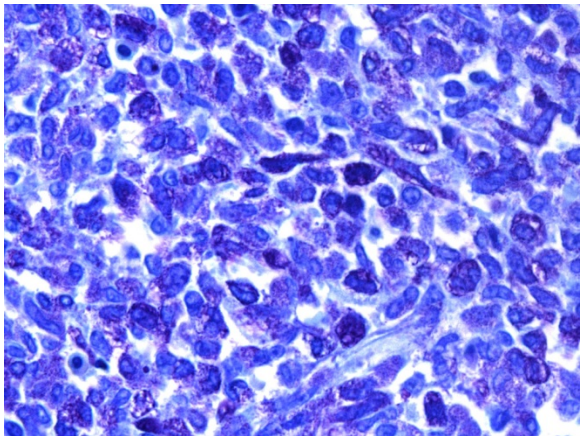

Thymus, rat. Neoplastic cells contain numerous metachromatic granules within their cytoplasm. (Toluidine blue, 400X). (Photo courtesy of: Laboratory of Pathology, Faculty of Pharmaceutical Sciences , Setsunan University, 45-1 Nagaotohge-cho, Hirakata, Osaka 573-0101, Japan http://www.setsunan.ac.jp/~p-byori/)

tumor difficult to differentiate from thymoma. Negative immunohistochemical staining for cytokeratin AE1/AE3 helps to rule out a thymoma in this rat. Granular cell tumors and globule leukocyte tumors are characterized as round cell tumors with eosinophilic granules, similar to those observed in the current case. Accordingly, metachromasia, using toluidine blue, was required to confirm the diagnosis.[2,7,9,12]

The thymic region of the tumor described here is composed of two areas with different densities, as well as different epithelial cell and lymphocyte morphologies, suggesting that cortical and medullary thymic components may have been maintained in the tumor. In humans, cortical and medullary thymic epithelial cells yield different expression patterns of cytokeratin. Medullary thymic epithelial cells express cytokeratin 5 and cytokeratin 14, whereas cortical thymic epithelial cells express cytokeratin 8 and cytokeratin 18.[5,11] Accordingly, immunohistochemical staining for different cytokeratins distinguishes between the cortex and the medulla of the thymus.

In this study, the expression patterns of cytokeratins 8 and 14 were analyzed in thymic epithelial cells of a normal RCS rat and shown to be similar to those observed in humans. Cytokeratins 8 and 14 were thus considered suitable markers for distinguishing between the cortex and medulla in RCS rats. In the RCS rat described here, the distribution of cytokeratins 8 and 14 corresponded to the areas with high and low epithelial cell densities, respectively. It was clear that the thymic area possessed both cortical and medullary components but that the epithelial cell density differed from that of the normal thymus. However, growth of solid tubules and epithelial cords, which represent a characteristic feature of benign thymoma, is not observed in our case. The area exhibiting high epithelial cell density represented the cortical component of the tumor with thymic epithelial hyperplasia; accordingly, this region was diagnosed as thymic epithelial hyperplasia. In our laboratory, we previously detected only one benign thymoma in about 20 RCS rats of over 120 weeks of age; however, almost all thymus showed severe involution. Therefore, this

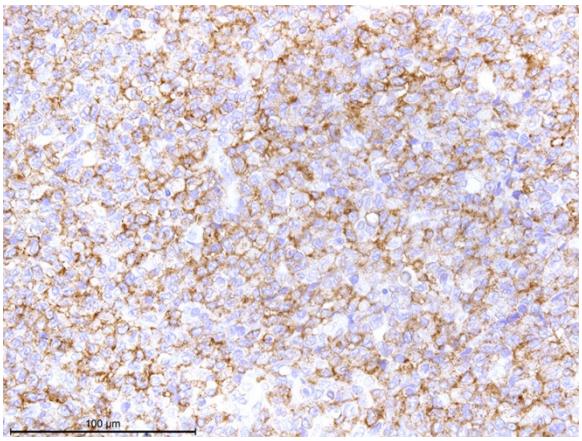

Thymus, rat. Neoplastic cells exhibit strong membranous positivtity for c-kit. (anti-c-kit, 400X). (Photo courtesy of: Laboratory of Pathology, Faculty of Pharmaceutical Sciences, Setsunan University, 45-1 Nagaotohge-cho, Hirakata, Osaka 573-0101, Japan http://www.setsunan.ac.jp/~p-byori/)

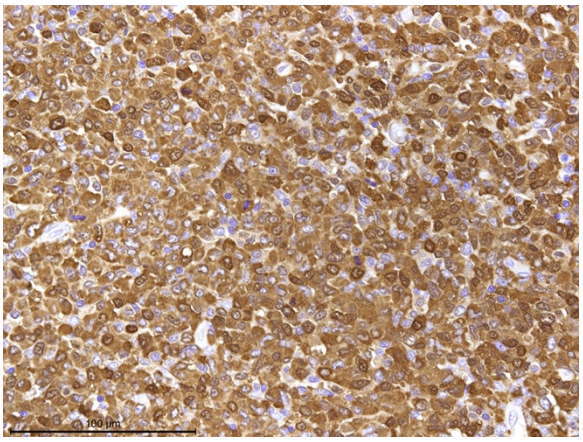

Thymus, rat. Neoplastic cells exhibit strong cytoplasmic positivity for rat mast cell protease. (anti-MCP, 400X). (Photo courtesy of: Laboratory of Pathology, Faculty of Pharmaceutical Sciences, Setsunan University, 45-1 Nagaotohge-cho, Hirakata, Osaka 573-0101, Japan http://www.setsunan.ac.jp/~p-byori/)

strain may not be prone to the development of thymic epithelial hyperplasia and thymoma.

JPC Diagnosis: Thymus: Mast cell tumor, RCS rat, *Rattus norvegicus*.

Conference Comment: Conference participants had great difficulty with the diagnosis and tissue identification in this case. While most attendees agreed that this case represented a malignant round cell neoplasm, none had mast cell tumor as a differential or thymus as the affected tissue. The neoplasm effaces the majority of the tissue; however, normal thymic parenchyma is present at the periphery of all examined tissue sections. As a result, the conference moderator led a discussion of the anatomical features of the rodent thymus.

The thymus is located in the mediastinum, cranial and ventral to the base of the heart and aortic arch with extension into the cervical region in the rat. It consists of two bilateral lobes joined by a connective tissue isthmus. Within the lobe, a thin capsule surrounds each lobule and gives rise to septae; however, septation is not apparent in this section.[10,11]

The thymus is unique among the lymphoid organs because it is supported by an epithelial framework, highlighted by the contributor's cytokeratin immuno-histochemical stains. It is divided into a cortex and medulla separated by a vascular corticomedullary zone. Histologically, the darkly staining cortex contains densely packed, small, immature T-lymphocytes, which obscure the epithelial cell population.[10,11] The medulla is less densely cellular than the cortex, and contains more mature T-cells, prominent epithelial cells, macrophages, dendritic cells, and B

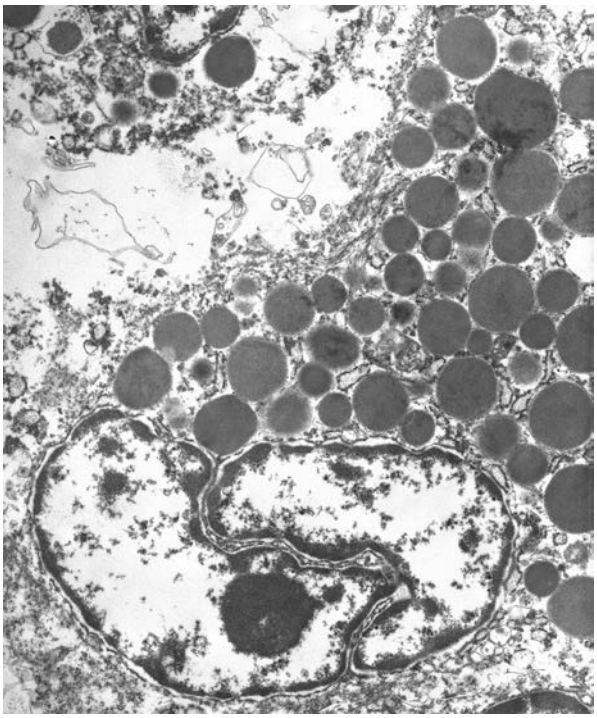

Thymus, rat. Neoplastic mast cells exhibit an indented nucleus, moderate amounts of round endoplasmic reticulum, and numerous variably-sized membrane-bound granules with granular contents. (Photo courtesy of: Laboratory of Pathology, Faculty of Pharmaceutical Sciences, Setsunan University, 45-1 Nagaotohge-cho, Hirakata, Osaka 573-0101, Japan http://www.setsunan.ac.jp/~p-byori/)

lymphocytes. Hassall's corpuscles are rare in rodents when compared with many other species, contributing to the difficulty participants had in tissue identification. In addition, given the age of this rat, the tissue is likely in an advanced stage of involution, further obscuring the normal architecture.[10,11]

Neoplastic cells in this section have numerous prominent pale eosinophilic cytoplasmic granules which are inconsistent with the deeply basophilic granules seen in well-granulated mast cell tumors in dogs and cats, as well as in normal rat mast cells. Conference participants considered other differentials including undifferentiated malignant round cell neoplasm, granular cell tumor, oncocytoma, balloon cell melanoma, and large granular lymphoma. In addition to the histochemical and immunohistochemical stains mentioned by the contributor that support the diagnosis of mast cell tumor, the provided transmission electron microscopy (TEM) image nicely demonstrates numerous intracytoplasmic homogenous electron dense granules consistent with mast cell granules.

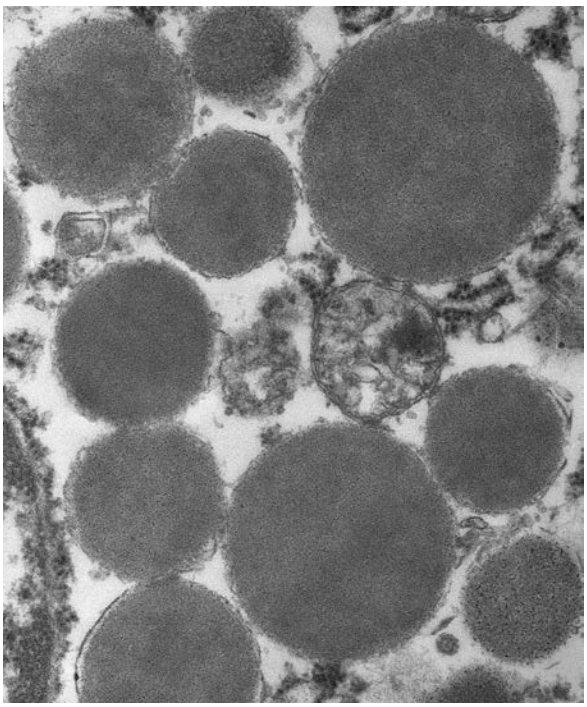

Thymus, rat. Higher magnification of the membrane-bound granules demonstrates that their contents are densely granular. A single mitochondria is present among them. (Photo courtesy of: Laboratory of Pathology, Faculty of Pharmaceutical Sciences, Setsunan University, 45-1 Nagaotohge-cho, Hirakata, Osaka 573-0101, Japan http://www.setsunan.ac.jp/~p-byori/)

Contributing Institution:
Laboratory of Pathology
Faculty of Pharmaceutical Science
Setsunan University,
Hirakata, Osaka, Japan
http://www.setsunan.ac.jp/~p-byori/

References:

1. Amihai D, Trachtenburg S, et al. The structure of mast cell secretory granules in the blind mole rat (*Spalax ehrenbergi*). *J Struct Biol*. 2001; 136:96-100.
2. Baselmans AH, Kuijpers MH, van Dijk JE. Brief communication: Histopathology of a spontaneously developing mast cell sarcoma in a Wistar rat. *Toxicol Pathol*. 1996; 24: 365-369.
3. Haseman JK, Hailey JR, Morris RW. Spontaneous neoplasm incidences in Fischer 344 rats and B6C3F1 mice in two-year carcinogenicity studies: A National Toxicology Program update. *Toxicol Pathol*. 1998; 26: 428-441.
4. Hosseini E, Pedram B, Bahrami AM, Moghaddam MH, Javanbakht J, Ghomi FE, Moghaddam NJ, Koohestani M, Shafiee R. Cutaneous mast cell tumor (mastocytoma): Cyto- histopathological and haematological investigations. *Diagn Pathol*. 2014; 9:9.
5. Lee EN, Park JK, Lee JR, Oh SO, Baek SY, Kim BS, Yoon S.

Characterization of the expression of cytokeratins 5, 8, and 14 in mouse thymic epithelial cells during thymus regeneration following acute thymic involution. *Anat Cell Biol*. 2011; 44:14-24.
6. Misdorp W. Mast cells and canine mast cell tumors: A review. *Vet Q*. 2004; 26:156-169.
7. Miyajima R, Hosoi M, Yamamoto S, Mikami S, Yamakawa S, Iwata H, Enomoto M. Eosinophilic granulated cells comprising a tumor in a Fischer rat. *Toxicol Pathol*. 1999; 27:233-236.
8. Miyakawa Y, Sato SI, Kakimoto K, Takahashi M, Hayashi Y. Induction of cutaneous mast cell tumors by N-methyl-N'-nitro-N-nitrosoguanidine followed by TPA in female mice of 4 out of 5 strains tested. *Cancer Lett*. 1990; 49:19-24.
9. Nagatani M, Nakamura A, Yamaguchi Y, Aikawa T, Tamura K. Spontaneous eosinophilic granulated round cell tumors in rats. *Vet Pathol*. 2001; 38:317-324.
10. Pearse G. Normal structure, function, and histology of the thymus. *Toxicol Pathol*. 2006; 34:504-514.
11. Sun L, Li H, Luo H, Zhao Y. Thymic epithelial cell development and its dysfunction in human diseases. *Biomed Res Int*. 2014; 206929.
12. Yamagishi Y, Katsuta O, Tsuchitani M. Mastocytoma in a Fischer 344 rat. *J Vet Med* Sci. 1992; 54:783-785.

CASE IV: MS15-5586 (JPC 4087116).

Signalment: One-month-old female Taconic line 8440 mouse (*Mus musculus*).

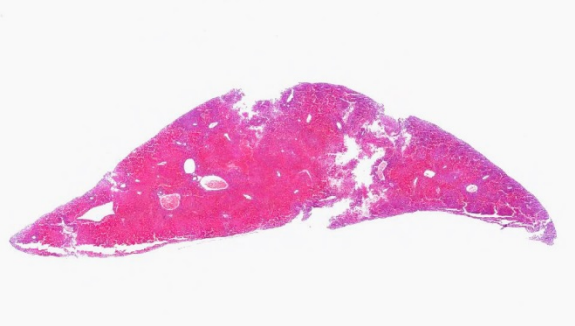

Liver, mouse. A single cross-section of the liver is presented for examination. (HE, 4X)

History: Four mice were presented dead. Three were found dead and one was euthanized prior to submission. According to the history, they were treated with azoxymethane.

Gross Pathology: All mice have congested livers with light brown apical margins.
Heart and kidneys are pale. The mice that were euthanized had blood tinged intestinal contents.

Laboratory results: Bacteriology*:* Small Intestine: *Enterococcus faecalis*, *Staphylococcus sciuri*, and *E. coli*; Negative for strict anaerobes.

Histopathologic Description: The liver has severe congestion of hepatic lobules with attenuation and loss of centrilobular hepatocytes. Portal zone hepatocytes are spared but have variably vacuolated cytoplasm.

Other histology findings include lymphocytolysis of the thymus. The mouse with intestinal hemorrhage has gastric ulcers. One mouse has necrosis of the adrenal cortex.

Contributor's Morphologic Diagnosis: Liver: Centrilobular to mid-zonal necrosis, and hemorrhage, severe, acute; micro-vesicular lipidosis mild to moderate

Contributor's Comment: Azoxymethane (AOM) is derived from the cycad palm nut of Guam. Ingestion has been associated with acute liver failure in cattle.[1]

In mice and rats, it is used as a mutagen in the study of colon carcinogenesis and liver failure. It is an alkylating agent that forms 06-methylguanine (0^6meG) adducts in DNA. 0^6meG formation has been found in human colon cancers. In the liver, AOM is oxidized to methylazoxymethanol by cytochrome P450 2E1 and transported to the colon where it methylates DNA which can cause G:C to A:T transition mutations.[2,3] Methylazoxymethanol is also associated with acute and chronic liver toxicity.[4]
At reported doses of 100 ug/g in mice AOM causes acute liver injury. It is characterized by hepatic necrosis and microvesicular lipidosis. The mechanism of action may be interference with beta-oxidation of fatty acids in the mitochondria[1] Hemorrhage is an indication of damage to sinusoidal endothelial cells.[4] Hepatic necrosis then progresses to liver failure and hepatic encephalopathy.

Acute liver failure is thought to lead to death via neurologic effects and hypotensive shock with multi-organ failure. Neurologic effects were thought to be a result of ammonia and other metabolites directly causing hepatic encephalopathy. More recent work has shown that inflammation-associated cytokine release contributes to brain edema and other clinical signs. Acute liver failure can result in cytokine storms with increased TNF-α, IL-1b, Il-6, and Il-12, There is also evidence of impaired neutrophil phagocytic activity and increased the risk of sepsis. Portal hypertension may cause increased bacterial translocation[5] cross the gut.[5, 6, 7]

JPC Diagnosis: Liver: Necrosis and hemorrhage, centrilobular to midzonal, acute, diffuse, severe with microvesicular

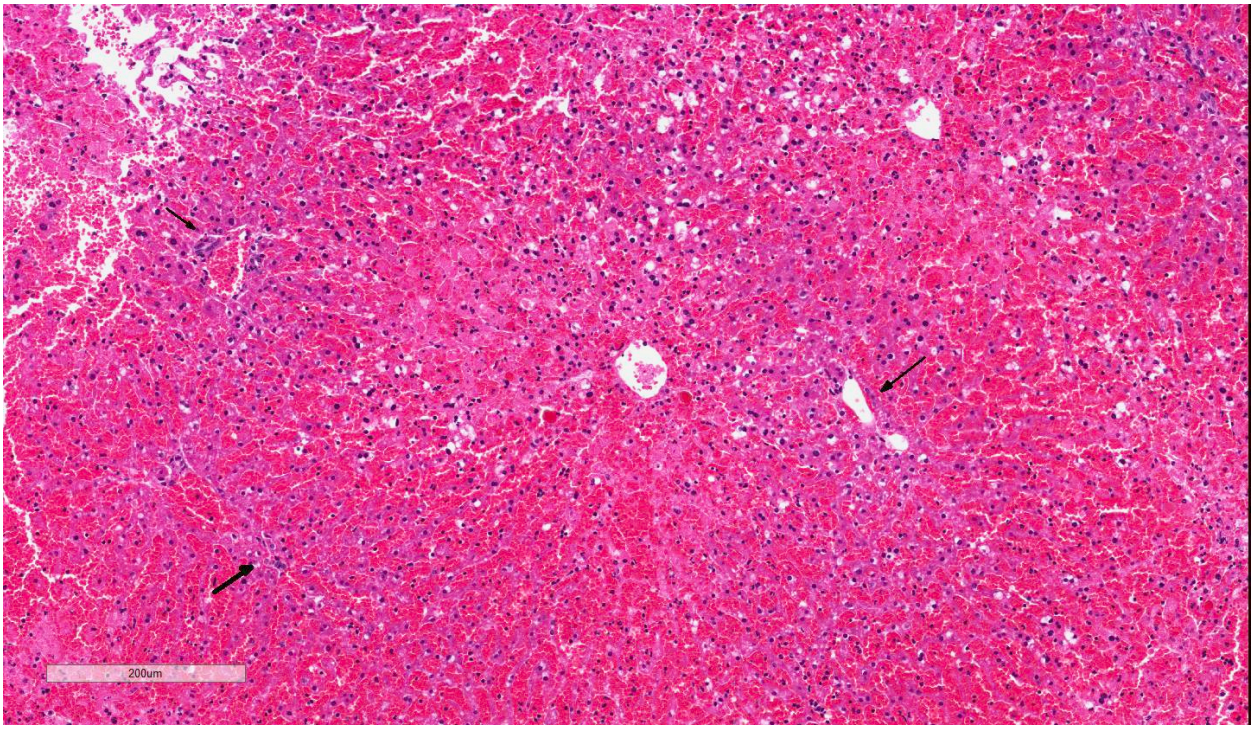

Liver, mouse. Hepatocellular architecture is diffusely lost, and there is diffuse hemorrhage within the centrilobular and midzonal areas. Portal areas are delimited by arrows. (HE, 63X)

lipidosis, Taconic line 8440 mouse, *Mus musculus*

Conference Comment: Despite some minor slide variability, the contributor provides a good example of the relatively stereotypical histologic changes associated with acute toxic hepatic injury. The liver is particularly susceptible to toxic injury due to constant exposure to ingested chemicals through the portal blood.[4] Additionally, hepatocytes are responsible for the metabolism of most endogenous and exogenous substances, by a process called biotransformation. This process is broken down into three phases based on the hepatic enzymes involved. Phase I reactions involve oxidation, reduction, hydrolysis, cyclization, and decyclization of the compound via cytochrome P450 monooxygenases (CYP) utilizing NADPH and oxygen in the smooth endoplasmic reticulum of hepatocytes. Phase II involves conjugation of the metabolite produced in phase I via glucuronidation, sulphation, acetylation, or methylation, ultimately resulting in a water soluble metabolite that is then excreted through urine or bile. Phase III reactions involve transporting the conjugated substances through the hepatocyte and into the bile canaliculus.[4,5,7]

Conference participants discussed the various mechanisms of hepatotoxic liver injury, which are divided into six categories based on the mechanism of action and cellular targets of the toxin.[4] The most common mechanism involves biotransformation of indirect-acting toxins by the CYP system, whichresults in bioactivated toxic metabolites that disrupt intracellular enzymatic pathways. CYP is abundant in the microsomes of the smooth endoplasmic reticulum in centrilobular zones which explains the prevalence of centrilobular to midzonal necrosis in some

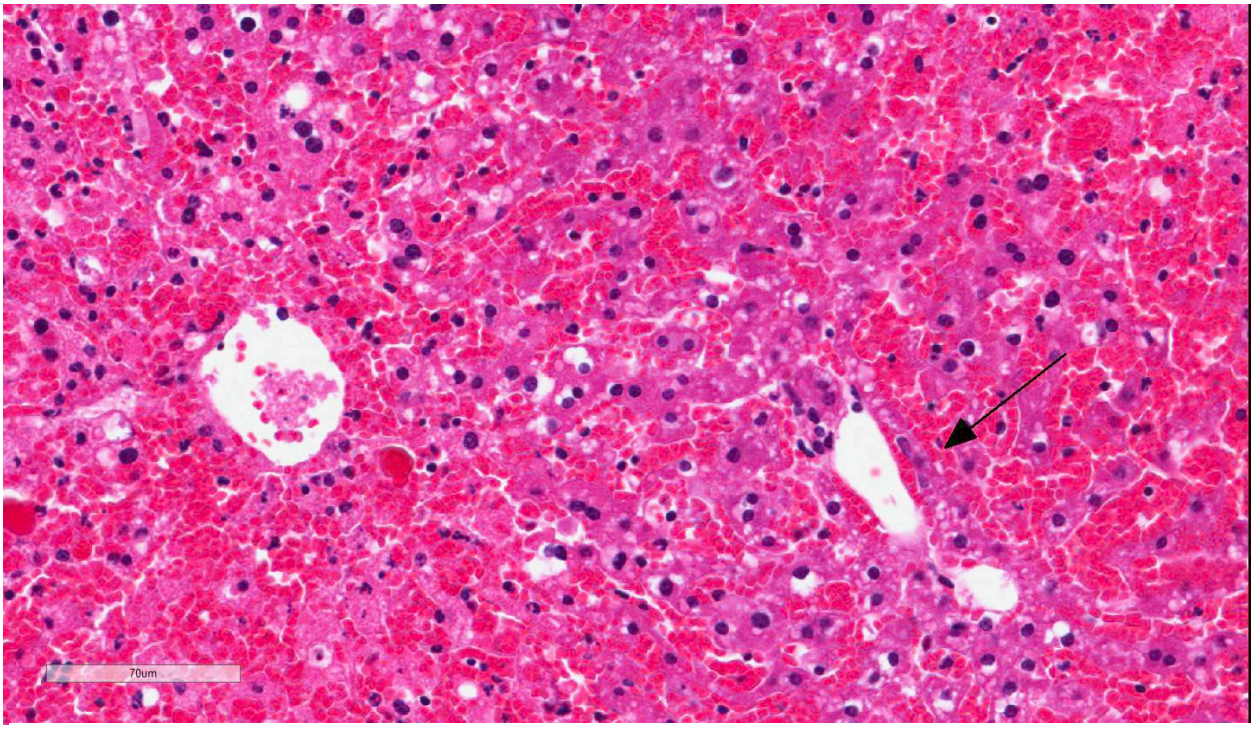

Liver, mouse. Hepatocytes within the centrilobular and midzonal areas of the lobule are shrunken and fragmented, with pyknotic or rrhectic nuclei, and there is marked hemorrhage in this area. A thin rim of viable hepatocytes, compressed by the marked congestion is present in portal areas. (HE, 224X)

toxic hepatopathies, including this case of azoxymethane toxicosis.[1,4,6] There is also inhibition of hepatic mitochondrial function, thus limiting beta-oxidation of fat and ATP generation via oxidative phosphorylation. This inhibition eventually leads to necrosis (due to production of damaging reactive oxygen species and lactic acid), as well as hepatocellular microvesicular lipid accumulation, as seen adjacent to areas of necrosis in this case.[4] Readers are encouraged to review 2012 WSC Conference 18 Case 2 for further discussion of other mechanisms of hepatotoxic liver injury.

In addition to hepatic necrosis, acute and fatal hepatotoxicity causes destruction of the endothelium of the sinusoidal lining cells, resulting in zonal areas of hemorrhage. Widespread hemorrhage is often associated with acute hepatocellular toxicity due to consumption of platelets and decreased production of clotting factors by the liver.[4] Centrilobular necrosis is the most common form of zonal hepatocellular necrosis observed in animals and may be caused by a variety of infectious, inflammatory, metabolic, and toxic insults. Although conference participants could not identify azoxymethane as the cause of the lesions in this mouse, most suspected a toxic etiology based upon the presence of centrilobular necrosis and hemorrhage combined with the lack of evidence of an infectious etiology.

Contributing Institution:
National Institutes of Health
Diagnostic and Research Services Branch
Division of Veterinary Resources
Bethesda, MD, 2892
https://www.nih.gov/

References:

1. Belanger M, et al. Neurobiological characterization of an azoxymethane mouse model of acute liver failure. *Neurochem Int.* 2006; (48):434-440.
2. Nyskolus LS, et al. Repair and removal of azoxymethane-induced 0^6-methyguanine in rat colon by0^6-methyguanine DNA methyltransferase and apoptosis. *Mutat Res*. 2013; 758: 80-86.
3. Sohn OS, et al. Metabolism of azoxymethane, methylazoxymethanol and N-nitrosodimethylamine by cytochrome p450IIE1. *Carcinogenesis*. 1991; 12 (1):127-131.
4. Stalker MJ, Cullen JM. Liver and biliary system, In: Maxie MG, ed. *Jubb, Kennedy and Palmer´s. Pathology of Domestic Animals.* Vol 2. 6th ed. St Louis, MO: Elsevier Saunders; 2016:325-330.
5. Tranah TH, et al. Systemic inflammation and ammonia in hepatic encephalopathy. *Metab Brain Dis*. 2013; 28:1-5.
6. Bemeur C, Desjardins P, Butterworth RF. Antioxidant and anti-inflammatory effects of mild hypothermia in the attenuation of liver injury due to azoxymethane toxicity in the mouse. *Metab Brain Dis*. 2010; 25:23-29.
7. Chastre A, et al. Inflammatory cascade driven by tumor necrosis factor-alpha play a major role in the progression of acute liver failure and its neurologic complications. *PLoS One*. 2012; 7(11):e49670.